PERGAMON

Micron 33 (2002) 687–691

micron

www.elsevier.com/locate/micron

Short communication

Measuring the aspect ratios of ZnO nanobelts

Yolande Berta, Christopher Ma, Zhong L. Wang*

School of Materials Science and Engineering, Georgia Institute of Technology, Atlanta, GA 30332-0245, USA

Received 20 May 2002; revised 18 July 2002; accepted 25 July 2002

Abstract

Nanobelts are new materials that have a rectangular cross-section and are characterized by widths and width-to-thickness aspect ratios. In this paper, the thickness and aspect ratios of ZnO nanobelts are measured by a conjunction application of convergent beam electron diffraction (CBED) and electron energy-loss spectroscopy (EELS). The thicknesses of thicker nanobelts are first determined by CBED under two-beam diffracting condition, then they are used to determine the electron inelastic mean-free-path (MFP) length, which is 161 ± 15 nm for ZnO at 200 kV. The thicknesses of the thinner nanobelts are then determined by EELS using the calibrated MFP. The results show that the aspect ratio depends on conditions under which the sample was synthesized.

Keywords: Electron energy-loss spectroscopy; Nanobelts; Convergent beam electron diffraction

1. Introduction

One-dimensional nanostructures have attracted much interest in recent years due to their potential application in nanoelectronics. Recently, long ribbon-like nanostructures of semiconducting oxides, such as ZnO, SnO_2, Ga_2O_3 and CdO have been successfully synthesized in our laboratory using a physical vapor deposition technique (Pan et al., 2001). These structures have a rectangular cross-section, a uniform thickness and width, and their morphology is best described by a belt (or ribbon). The nanobelts differ from the more conventional nanowires in that they are almost void of dislocations and other line-defects, making them important for electronic and optoelectronic applications.

It is known that the properties of nanostructures depend strongly on their size and shape (Wang, 1999). The width of the nanobelts can be precisely determined by transmission electron microscopy, while the thickness of the nanobelts may not be directly given by the image unless a cross-section sample is prepared using ultramicrotomy techniques. In this paper, convergent beam electron diffraction (CBED) is applied to determine the thickness of relatively thick ZnO nanobelts. The measured thickness is then applied to determine the electron inelastic scattering mean-free-path length (MFP) (Λ) in conjuction with electron energy-loss spectroscopy (EELS). Using the t/λ value measured by EELS, the thickness, t, for relatively thinner nanobelts is determined. The results provide the width-to-thickness ratios of individual nanobelts and the correlation between thickness and width.

2. Experimental methods

The synthesis and microstructural characterization of the nanobelts have been reported in detail elsewhere (Pan et al., 2001). Fig. 1 shows a typical low-magnification TEM image of the ZnO nanobelts, clearly displaying a belt shape. The nanobelt has a uniform thickness and width, thus, it is an ideal sample for thickness measurement.

Our experimental measurements were carried out in three steps. The first step was to determine the thickness of the nanobelts. This procedure was achieved by CBED under two-beam diffracting condition. The details of the CBED procedure have been described by Allen (1981). For ZnO with wurtzite structure, the hexagonal crystalline sample was first tilted to the [0001] zone, as a reference for later indexing the CBED discs. Two-beam condition was then attained, with the help of Kikuchi lines observed under dynamical diffraction conditions. The convergent beam central and diffraction discs were recorded on film, and then

* Corresponding author. Tel.: +1-404-894-8008; fax: +1-404-894-9140.
E-mail address: zhong.wang@mse.gatech.edu (Z.L. Wang).

0968-4328/02/$ - see front matter
PII: S0968-4328(02)00026-4

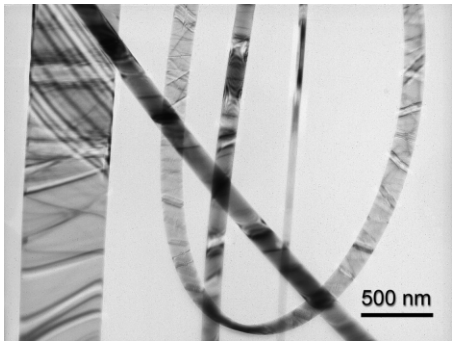

Fig. 1. Typical TEM image of ZnO nanobelts that exhibit a 'ribbon' geometry.

scanned into an electronic file for accurate measurement of the fringe positions. Using information within the parallel, symmetric fringes found in the chosen diffracted disk, the excitation error (s_i) for that disc was calculated using the following relation (see Fig. 2):

$$s_i = \frac{\Delta X}{X}\lambda g^2 \tag{1}$$

where λ is the wavelength of the incident electron beam, g the reciprocal hkl interplanar spacing, ΔX the measured distance between the central fringe and the ith fringe in the diffracted disc, X the distance between the central disk (000) and the diffracted disc.

Crystal thickness was then calculated from the equation first described by Kossel and Möllenstedt:

$$\frac{s_i^2}{n_i^2} + \frac{1}{\xi_g^2 n_i^2} = \frac{1}{t^2} \tag{2}$$

where s_i represents the excitation error for the ith fringe in the CBED disc, n_i is an integer for minima and a non-negative real number for maxima, ξ_g represents the extinction distance, and t the crystal thickness.

The values of n_i were determined by trial and error based on whether the plotted values s_i^2/n_i^2 vs. $1/n_i^2$ yielded the best-fit straight line. From the equation of the line, the y-intercept is equal to $1/t^2$ and the slope is $1/\xi_g^2$. Allen (1981) reported that this method of thickness determination had an error of $\pm 2\%$, for metals, if the (200), (220), (311) and higher order reflections are used. The accuracy for ceramics may be

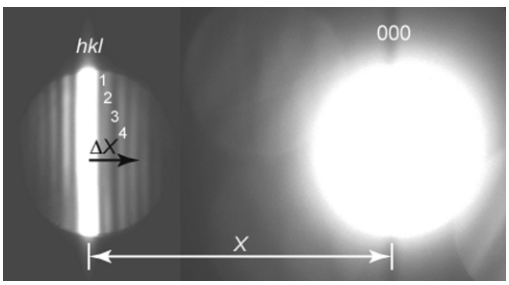

Fig. 2. Illustration of the measurements of X and ΔX in CBED.

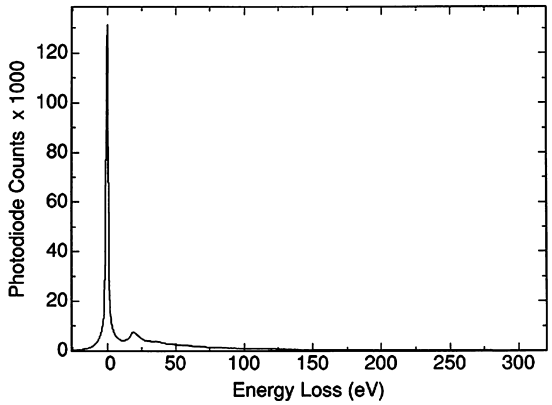

Fig. 3. A typical low-loss EELS spectrum acquired from a ZnO nanobelt at 200 kV.

higher due to less strain and deformation, as well as cleaner surfaces.

The second step was to measure the electron inelastic scattering MFP length, Λ. Simultaneous to the acquisition of the CBED pattern used for the thickness measurement in the first step, the EELS spectrum was acquired from the same area of the sample (Fig. 3), and t/Λ calculated from the relation, provided the plural scattering obeys the Poisson distribution law:

$$t/\Lambda = \ln(I_T/I_0) \tag{3}$$

where I_0 is the integrated intensity of the zero-loss peak, and I_T the integrated intensity of the entire EELS spectrum. In conjunction with the thickness measured from CBED, the electron inelastic MFP length can be determined. Calculations of the $\ln(I_T/I_0)$ were performed by EL/P software (Gatan, Inc., Warrendale, PA).

Due to the co-existence of several excitations such as surface plasmons and volume plasmon, the measured MFP is actually an effective MFP that is related to the MFPs of individual events by $1/\Lambda_T = 1/\Lambda_1 + 1/\Lambda_2 + \cdots$ Eq. (3) holds if: (1) the inelastically scattered electrons in all angular ranges are collected by EELS; and (2) there is no elastic scattering and diffraction effect. To meet the first condition, a large entrance aperture is required to avoid obvious error. It is believed that the EELS acquired in imaging mode without an objective aperture in our experiments should meet this criterion. As for the second condition, we know that diffraction and elastic scattering are inevitable in electron scattering. The calculation and experiments by Egerton and Wang (1990) have demonstrated that Eq. (3) is an excellent approximation for plasmon losses because the characteristic inelastic scattering angle is much smaller than the Bragg angle for elastic scattering.

Finally, to obtain the aspect ratio of nanobelts with a wide range of thicknesses, including those too thin to be measured by CBED, the experimentally measured MFP of the material was used to calculate the thickness of individual nanobelts based on the calculated t/Λ value from the

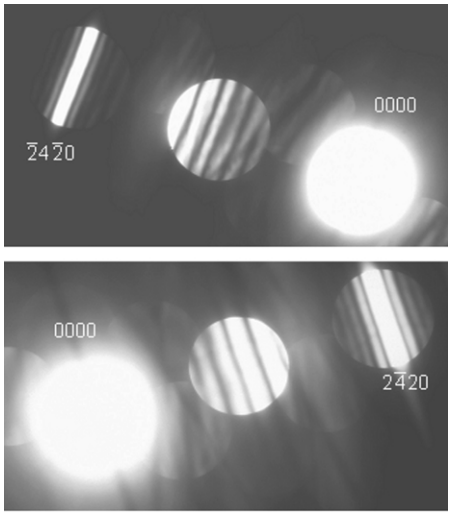

Fig. 4. Two CBED patterns taken from the same nanobelt under two-beam diffracting conditions, which will be used independently for thickness measurements.

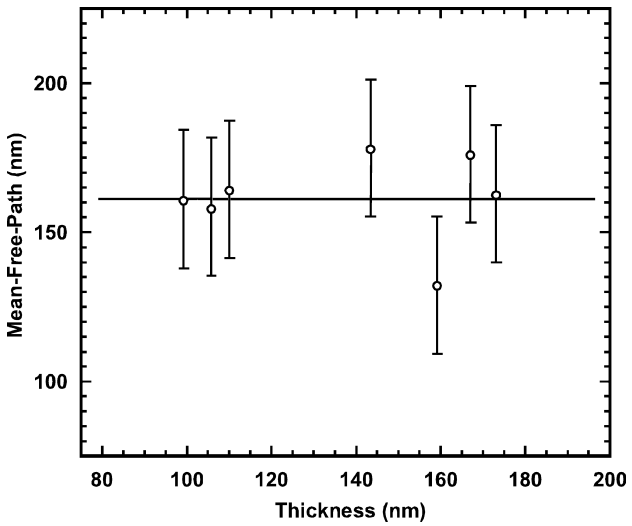

Fig. 6. Plot of experimentally determined mean free path (λ) values for individual nanobelts versus thickness, showing the data consistency and the independency of λ of the thickness of the nanobelts.

acquired EELS spectra. The widths of the nanobelts were measured directly from TEM micrographs.

The CBED experiments were carried out at 200 kV using a Hitachi HF2000 FEG TEM, which is equipped with a Gatan parallel detection EELS. The energy resolution of the EELS was 1.0 eV. All of the EELS spectra were acquired in imaging mode without the presence of an objective aperture, thus, the collection angle was rather large. The EELS data were acquired at 0.3 eV/ch for an energy range of 250 eV above the zero-loss.

3. Experimental results

Thickness measurement using CBED is more precise for thicker nanobelts showing dynamical diffraction contrast. Thus, we deliberately selected nanobelts with larger thickness values. For a single nanobelt, thickness can be determined under two-beam diffracting conditions with any of several diffracted beams (Fig. 4). To confirm the accuracy of thickness determination by CBED for the nanobelts, three separate reflections, such as ($\bar{2}420$), ($4\bar{1}30$) and ($3\bar{2}50$), from the same nanobelt were used under two-beam diffracting conditions. The thickness was calculated for each Bragg reflection and compared to the other two. The thickness was accepted when the three values were within 10% of each other, and the electron inelastic MFP length was calculated using Eq. (3). Fig. 5 shows the s_i^2/n_i^2 vs. $1/n_i^2$ plot for three reflections that were acquired from the same nanobelt. It is apparent that the y-intercepts of the three reflections have similar values, indicating the consistency in thickness values. The different slopes of the three reflections originate from their different extinction distances, which depend on the corresponding structure factors for the selected Bragg

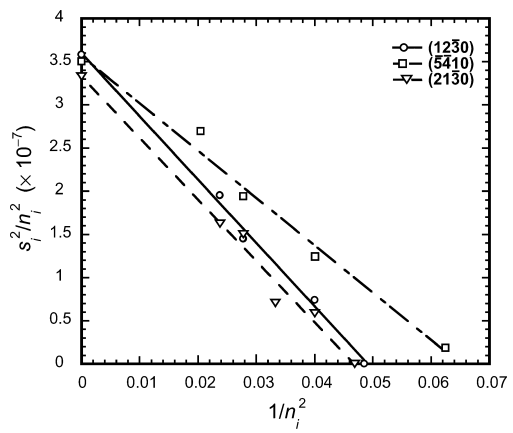

Fig. 5. s_i^2/n_i^2 vs. $1/n_i^2$ plot for three reflections acquired from the same nanobelt and their linear fits.

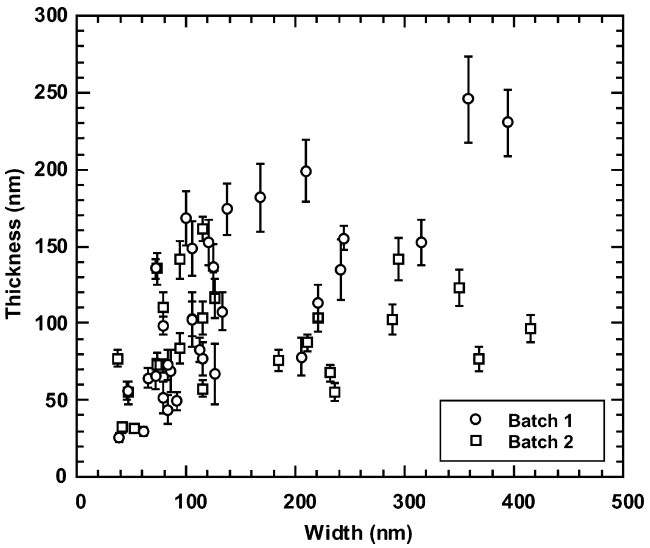

Fig. 7. Measured aspect ratios of nanobelts for two samples as a function of nanobelt widths.

beams. Therefore, as expected, thickness calculations from different g reflections for the same nanobelt converge to a single thickness value, but have different slopes for their respective extinction distances. We have confirmed this by comparing the extinction distances of the same reflections, recorded from different nanobelts. The values were within $\pm 15\%$ of each other.

After conducting a systematic and careful analysis of the data and ruling out artifacts, Fig. 6 gives the plot of the measured MFP vs. sample thickness, indicating that, within experimental error, the MFP is independent of thickness, as expected, because MFP is a quantity that is determined by the electronic structure of the material. The average MFP length for ZnO at 200 kV is 161 ± 15 nm. This value was taken as the reference for determining the thickness of thinner nanobelts.

Based on the measured MFP, the thickness and aspect ratio for the nanobelts with smaller dimensions were determined from the EELS data, based on Eq. (2), and the final results are plotted in Fig. 7. We have determined the aspect ratio for nanobelts synthesized under slightly different experimental conditions. For batch 1, the aspect ratios of width-to-thickness are ~ 1.2 for nanobelts less than 100 nm in width and 1.5 for those greater than 100 nm in widths. For batch 2, the aspect ratio is relatively high: between 3 and 4.

4. Discussion

The error for the measurements is an accumulation of both CBED and EELS techniques. Eq. (2) was derived under conditions neglecting both many-beam effects and absorption. In fact, the two-beam condition is hardly achieved for thin nanobelts because of the shape effect induced by the small sample thickness. We have tried to minimize the many-beam effect by selecting the diffraction discs having relatively large reciprocal vectors. Previous extensive investigation has shown that the many-beam effect can strongly affect the final results (Ecob, 1986), and it can lead to an error of up to 10% (Spence and Zuo, 1992). We do not believe that the selection of the initial value n_i can lead to a large error in our case, because we have measured the thickness of the same nanobelt using different diffracted beams, and the result was accepted only when all of the beams gave sample thickness values within 10% of each other.

The log-ratio technique for thickness measurement in TEM has been investigated by Malis et al. (1988). Eq. (3) is valid if there is mostly volume excitation, which means that the sample has to be relatively thick to ensure the dominant contribution from volume plasmon. The $\ln(I_T/I_0)$ technique can give an accuracy within 10% if the sample is relatively thick, in the range of $0.2 < t/\Lambda < 5$ (Hosoi et al., 1981; Leapman et al., 1984). The basis of $t/\Lambda = \ln(I_T/I_0)$ measurement assumes no angular broadening. But for thicker samples, the elastic scattering and change in angular distribution of the inelastic scattering due to plural scattering will give rise to an error in thickness measurement. For thin samples with $t/\lambda < 0.2$, however, the surface excitation may become very significant, resulting in about 10–15% overestimation of the thickness (Egerton, 1986). Therefore, the CBED-EELS method demonstrated here may not work well for nanobelts thinner than ~ 30 nm.

There are several approaches that have been developed for accurate measurement of thickness. The most accurate technique is probably by quantitative CBED, which relies on quantitative fitting of the rocking curve in the CBED pattern through full dynamic calculation with the inclusion of absorption effects (Zuo et al., 1988; Wu et al., 1999). For metallic specimens, the Sum-Rule method has also been demonstrated as an effective method for thickness measurement after surface correction (Egerton, 1986).

5. Conclusion

Nanobelts are characterized by widths, thickness and width-to-thickness aspect ratios. Due to the small size of the nanobelts, it is rather challenging to measure their thickness accurately. In this paper, we have presented a technique for measuring the thickness and width-to-thickness aspect ratios of ZnO nanobelts by a conjunction application of CBED and EELS. The analysis consisted of three steps. First, the thickness of thicker nanobelts are determined by CBED under two-beam conditions, because CBED is best for crystals that are thicker than the extinction distances. In the second step, the measured thickness is used to determine the electron inelastic (MFP) length based on the EELS data recorded from the same nanobelt. Finally, the thicknesses of the thinner nanobelts are determined by EELS using the calibrated MFP. Our analysis shows that the MFP for ZnO is 161 ± 15 nm at 200 kV. The width-to-thickness aspect ratio of ZnO nanobelts is 1.2–3, depending on the width, as well as the synthesis conditions.

Acknowledgements

Thanks to Dr Z.R. Dai for many stimulating discussions and Dr Z.W. Pan for supplying the ZnO specimen. This research was supported by the NSF grants DMR-9733160 and Georgia Tech. Chris Ma thanks the fellowship from the Georgia Tech Molecular Design Institute, under the prime contract N00014-95-11116 from the Office of Naval Research.

References

Allen, S.M., 1981. Foil thickness measurements from convergent-beam diffraction patterns. Phil. Mag. A 43, 325–335.

Ecob, R.C., 1986. Comments on the measurement of foil thickness by convergent beam electron diffraction. Scr. Metall. 20, 1001.

Egerton, R.F., 1986. Electron Energy-Loss Spectroscopy in the Electron Microscope, Plenum Press, New York, Section 5.1.

Egerton, R.F., Wang, Z.L., 1990. Plural-scattering deconvolution of electron energy-loss spectra recorded with an angle-limiting aperture. Ultramicroscopy 32, 137–148.

Hosoi, J., Oikawa, T., Inoue, M., Kokubo, Y., Hama, K., 1981. Measurement of partial specific thickness (net thickness) of critical-point-dried cultured fibroblast by energy analysis. Ultramicroscopy 7, 147–154.

Leapman, R.D., Fiori, C.E., Swyt, C.R., 1984. Mass thickness determination by electron energy-loss for quantitative X-ray microanalysis in biology. J. Microsc. 133, 239–253.

Malis, T., Cheng, S.C., Egerton, R.F., 1988. EELS log-ratio technique for specimen-thickness measurement in the TEM. J. Electron Microsc. Tech. 8 (2), 193–200.

Pan, Z., Dai, Z., Wang, Z., 2001. Nanobelts of semiconducting oxides. Science 291, 1947–1949.

Spence, J.C.H., Zuo, J.M., 1992. Electron Microdiffraction, Plenum Press, New York, Section 4.1.

Wang, Z.L., 1999. Characterization of Nanophase Materials, Wiley/VCH, Weinheim.

Wu, L., Zhu, Y., Tafto, J., 1999. Towards quantitative measurements of charge transfer in complex crystals using imaging and diffraction of fast electrons. Micron 30 (5), 357–369.

Zuo, J.M., Spence, J.C.H., O'Keefe, M., 1988. Bonding in GaAs. Phys. Rev. Lett. 61, 353–356.